Inorg. Chem. **2002**, *41*, 6062–6070

Peculiar Antiaromatic Inorganic Molecules of Tetrapnictogen in $Na^+Pn_4^-$ (Pn = P, As, Sb) and Important Consequences for Hydrocarbons

Aleksey E. Kuznetsov,[†] Hua-Jin Zhai,[‡,§] Lai-Sheng Wang,*[,‡,§] and Alexander I. Boldyrev*[,†]

Department of Chemistry and Biochemistry, Utah State University, Logan, Utah 84322, Department of Physics, Washington State University, 2710 University Drive, Richland, Washington 99352, and W. R. Wiley Environmental Molecular Sciences Laboratory, Pacific Northwest National Laboratory, MS K8-88, P.O. Box 999, Richland, Washington 99352

Received June 25, 2002

Although aromaticity has been observed in inorganic and all-metal species, the concept of antiaromaticity has not been extended beyond organic molecules. Here, we present theoretical and experimental evidence that the 6 π-electron tetrapnictogen dianions in $Na^+Pn_4^{2-}$ (Pn = P, As, Sb) undergo a transition from being aromatic to antiaromatic upon electron detachment, yielding the first inorganic antiaromatic $Na^+Pn_4^-$ molecules. Two types of antiaromatic structures were characterized, the conventional rectangular species and a new peculiar quasiplanar rhombus species. Aromaticity and antiaromaticity in the tetrapnictogen molecules were derived from molecular orbital analyses and verified by experimental photodetachment spectra of $Na^+Pn_4^{2-}$. On the basis of our findings for the tetrapnictogen clusters, we predicted computationally that the organic $C_4H_4^-$ anion also possesses two antiaromatic structures: rectangular and rhombus. Moreover, only the rhombus antiaromatic minimum was found for the radical NC_3H_4, thus extending the peculiar rhombus antiaromatic structure first uncovered in inorganic clusters into organic chemistry.

Introduction

Heavier main group elements are known to form polyanionic clusters and networks in the solid state, and their electronic and geometric structures are usually explained on the basis of the Wade's rules. That is very different from planar hydrocarbons and their derivatives, whose electronic structures are usually explained on the basis of the concept of aromaticity. In recent years, these two different ideas started to merge: whereas the concept of aromaticity was extended into inorganic molecules, 3D-deltahedra-type structures (such as tetrahedrons, cubes, and the famous buckyball), characteristic of inorganic clusters, were found in organic chemistry. However, despite the fact that inorganic aromatic molecules have been identified, antiaromatic inorganic molecules have not been observed, which makes the aromaticity concept in inorganic chemistry incomplete. In this study, we present theoretical and experimental evidence that the tetrapnictogen dianions in $Na^+Pn_4^{2-}$ (Pn = P, As, Sb) undergo a transition from being aromatic to antiaromatic upon electron detachment, yielding the first inorganic antiaromatic $Na^+Pn_4^-$ molecules.

Hydrocarbons provide us with good references of aromatic and antiaromatic molecules. Whereas cyclobutadiene (C_4H_4) with only 4 π-electrons is a well-characterized antiaromatic molecule with a rectangular carbon framework, the $C_4H_4^{2-}$ dianion is known to be an aromatic molecule with 6 π-electrons, and it has been synthesized in the form of $Li_2C_4H_4$ ($Li^+{}_2C_4H_4^{2-}$).[1−3] Though C_4H_4 also has a tetrahedral isomer, it is 25 kcal/mol less stable than the antiaromatic planar structure.[1] The tetrapnictogens (Pn_4) and its dianions (Pn_4^{2-}) are valent isoelectronic with C_4H_4 and $C_4H_4^{2-}$, respectively, and thus, they present an excellent opportunity to examine aromaticity and, in particular, antiaromaticity in inorganic species. However, just like $C_4H_4^{2-}$, the Pn_4^{2-} species were not expected to be electronically stable gaseous species without counterions. To produce them and probe

* To whom correspondence should be addressed. E-mail: ls.wang@pnl.gov (L.S.W.); boldyrev@cc.usu.edu (A.I.B.).
[†] Utah State University.
[‡] Washington State University.
[§] Pacific Northwest National Laboratory.

(1) Balci, M.; McKee, M. L.; Schleyer, P. v. R. *J. Phys. Chem. A* **2000**, *104*, 1246.
(2) van Zandwijk, G.; Janssen, R. A. J.; Buck, H. M. *J. Am. Chem. Soc.* **1990**, *112*, 4155.
(3) Sekiguchi, A.; Matsuo, T.; Watanabe, H. *J. Am. Chem. Soc.* **2000**, *122*, 5652.

10.1021/ic020426+ CCC: $22.00
Published on Web 10/22/2002

them experimentally, at least one counterion would be required to stabilize them in the form of a singly charged anion, $M^+Pn_4^{2-}$, which would also be convenient for mass analyses and photodetachment experiments.

As we showed previously,[4,5] photodetachment photoelectron spectroscopy (PES) combined with ab initio calculations is a powerful means to obtain detailed information about the structure and bonding of novel gaseous clusters. In the present work, we obtained the PES spectra of a series of $NaPn_4^-$ (Pn = P, As, Sb) species. Well-resolved PES features were observed for all three molecules and compared with theoretical calculations to explore the idea of antiaromaticity in inorganic species.

Experimental Method

Details of the experimental apparatus have been described previously.[6,7] The $NaPn_4^-$ (Pn = P, As, Sb) species were produced by laser vaporization of mixed targets between the corresponding pnictogens and NaN_3. The latter was used as the source of sodium to produce Na-containing clusters. Various mixed clusters were produced from the cluster source and were mass analyzed using a time-of-flight mass spectrometer. The appropriate $NaPn_4^-$ species were mass-selected and decelerated before being photodetached. Three detachment photon energies were used in the current experiment, 355 nm (3.496 eV), 266 nm (4.661 eV), and 193 nm (6.424 eV). The photoelectron spectra were calibrated using the known spectrum of Cu^-, and the resolution of the apparatus was better than 30 meV for 1 eV electrons.

Theoretical Methods

We initially optimized geometries and calculated frequencies of Pn_4, Pn_4^-, Pn_4^{2-}, $NaPn_4^-$, and $NaPn_4$ (Pn = P, As, Sb) using analytical gradients with polarized split-valence basis sets (6-311+G*)[8−10] for Na, P, and As, pseudopotentials describing core electrons and the valence (CEP-121G) basis sets extended by a set of s-, p-, and d-functions ($\alpha_{s,p} = 0.0193$; $\alpha_d = 0.216$) for Sb and by a set of s-, p-, and d-functions ($\alpha_{s,p} = 0.0049$; $\alpha_d = 0.105$) for Na (CEP-121G+spd),[11−13] and a hybrid method known in the literature as B3LYP.[14−16] Then, we refined geometries and calculated frequencies at the second-order Møller−Plesset perturbation theory (MP2) level and the same basis sets.[17] Pn_4, Pn_4^-, Pn_4^{2-}, $NaPn_4^-$, and $NaPn_4$ (Pn = P, As) were further studied using the coupled-cluster method [CCSD(T)][18−20] with the 6-311+G* basis sets. Sb_4, Sb_4^-, Sb_4^{2-}, $NaSb_4^-$ and $NaSb_4$ were further studied using the coupled-cluster method [CCSD(T)] with the CEP-121G+spd basis sets. The energies of the most stable structures were refined using the CCSD(T) method and the more extended 6-311+G(2df) basis sets for Pn = P and As. The vertical electron detachment energies (VDEs) were calculated using the outer valence Green Function method[21−25] [OVGF/6-311+G(2df)] and CCSD(T)/6-311+G* geometries for $NaPn_4^-$ (Pn = P and As) and [OVGF/CEP-121G+spd] and CCSD(T)/CEP-121G+spd geometries for $NaPn_4^-$ (Pn = Sb). Core electrons were kept frozen in treating the electron correlation at the MP2, CCSD(T), and OVGF levels of theory except for MP2 calculations for Pn = P, where all electrons were included in correlation calculations (MP2(full)). All calculations were performed using the Gaussian 98 program.[26] MOs for C_4H_4, As_4, $C_4H_4^{2-}$, and As_4^{2-}, were calculated at the RHF/6-311+G* level of theory. All MO pictures were made using the MOLDEN 3.4 program.[27]

Experimental Results

Figure 1 shows the PES spectra of $NaPn_4^-$ (Pn = P, As, Sb) at three photon energies. Numerous well-resolved PES features were observed for each species, representing transitions from the $Na^+Pn_4^{2-}$ anions to the various states of the $Na^+Pn_4^-$ neutrals.

NaP_4^-. The spectral features of NaP_4^- were very broad. At 355 nm, two well-separated features (X and A) were observed; the A feature appeared to be cut off. The broad width of the X feature indicates that there must be a significant geometry change between the ground states of the anion and neutral species. A VDE of 2.52 eV was obtained for the ground state transition from the peak maximum of the X feature of the 355 nm spectrum. Because no vibrational structures were resolved for the X band, we estimated the adiabatic electron detachment energy (ADE) of NaP_4^- by drawing a straight line along the leading edge and adding a constant to the intersection with the binding energy axis to take into account the instrumental resolution

(4) Wang, L. S.; Boldyrev, A. I.; Li, X.; Simons, J. *J. Am. Chem. Soc*. **2000**, *122*, 7681.
(5) Li, X.; Kuznetsov, A. E.; Zhang, H. F.; Boldyrev, A. I.; Wang, L. S. *Science* **2001**, *291*, 859.
(6) Wang, L. S.; Cheng, H. S.; Fan, J. *J. Chem. Phys*. **1995**, *102*, 9480.
(7) Wang, L. S.; Wu, H. On *Advances in Metal and Semiconductor Clusters. IV. Cluster Materials*; Duncan, M. A., Ed.; JAI Press: Greenwich, CT, 1998; p 299.
(8) McLean, A. D.; Chandler, G. S. *J. Chem. Phys*. **1980**, *72*, 5639.
(9) Clark, T.; Chandrasekhar, J.; Spitznagel, G. W.; Schleyer, P. v. R. *J. Comput. Chem*. **1983**, *4*, 294.
(10) Frisch, M. J.; Pople, J. A.; Binkley, J. S. *J. Chem. Phys*. **1984**, *80*, 3265.
(11) Stevens, W. J.; Basch, H.; Krauss, J. *J. Chem. Phys*. **1984**, *81*, 6026.
(12) Stevens, W. J.; Krauss, J.; Basch, H.; Jasien, P. G. *Can. J. Chem*. **1992**, *70*, 612.
(13) Cundari, T. R.; Stevens, W. J. *J. Chem. Phys*. **1993**, *98*, 5555.
(14) Parr, R. G.; Yang, W. *Density-functional theory of atoms and molecules*; Oxford University Press: Oxford, 1989.
(15) Becke, A. D. *J. Chem. Phys*. **1993**, *98*, 5648.
(16) Perdew, J. P.; Chevary, J. A.; Vosko, S. H.; Jackson, K. A.; Pederson, M. R.; Singh, D. J.; Fiolhais, C. *Phys. Rev. B* **1992**, *46*, 6671.
(17) Krishnan, R.; Binkley, J. S.; Seeger, R.; Pople, J. A. *J. Chem. Phys*. **1980**, *72*, 650.
(18) Cizek, J. *Adv. Chem. Phys*. **1969**, *14*, 35.
(19) Purvis, G. D., III; Bartlett, R. J. *J. Chem. Phys*. **1982**, *76*, 1910.
(20) Scuseria, G. E.; Janssen, C. L.; Schaefer, H. F., III. *J. Chem. Phys*. **1988**, *89*, 7282.
(21) Cederbaum, L. S. *J. Phys B: At. Mol. Opt. Phys.* **1975**, *8*, 290.
(22) Niessen, W. von; Shirmer, J.; Cederbaum, L. S. *Comput. Phys. Rep*. **1984**, *1*, 57.
(23) Zakrzewski, V. G.; Niessen, W. von. *J. Comput. Chem*. **1993**, *14*, 13.
(24) Zakrzewski, V. G.; Ortiz, J. V. *Int. J. Quantum Chem*. **1995**, *53*, 583.
(25) For recent review see: Ortiz, J. V.; Zakrzewski, V. G.; Dolgunitcheva, O. In *Conceptual Trends in Quantum Chemistry*; Kryachko, E. S., Ed.; Kluwer: Dordrecht, 1997; Vol. 3, p 463.
(26) Frisch, M. J.; Trucks, G. W.; Schlegel, H. B.; Scuseria, G. E.; Robb, M. A.; Cheeseman, J. R.; Zakrzewski, V. G.; Montgomery, J. A., Jr.; Stratmann, R. E.; Burant, J. C.; Dapprich, S.; Millam, J. M.; Daniels, A. D.; Kudin, K. N.; Strain, M. C.; Farkas, O.; Tomasi, J.; Barone, V.; Cossi, M.; Cammi, R.; Mennucci, B.; Pomelli, C.; Adamo, C.; Clifford, S.; Ochterski, J.; Petersson, G. A.; Ayala, P. Y.; Cui, Q.; Morokuma, K.; Malick, D. K.; Rabuck, A. D.; Raghavachari, K.; Foresman, J. B.; Cioslowski, J.; Ortiz, J. V.; Stefanov, B. B.; Liu, G.; Liashenko, A.; Piskorz, P.; Komaromi, I.; Gomperts, R.; Martin, R. L.; Fox, D. J.; Keith, T.; Al-Laham, M. A.; Peng, C. Y.; Nanayakkara, A.; Gonzalez, C.; Challacombe, M.; Gill, P. M. W.; Johnson, B. G.; Chen, W.; Wong, M. W.; Andres, J. L.; Head-Gordon, M.; Replogle, E. S.; Pople, J. A. *Gaussian 98*, revision A.7; Gaussian, Inc.: Pittsburgh, PA, 1998.
(27) Schaftenaar, G. *MOLDEN3.4*; CAOS/CAMM Center: The Netherlands, 1998.

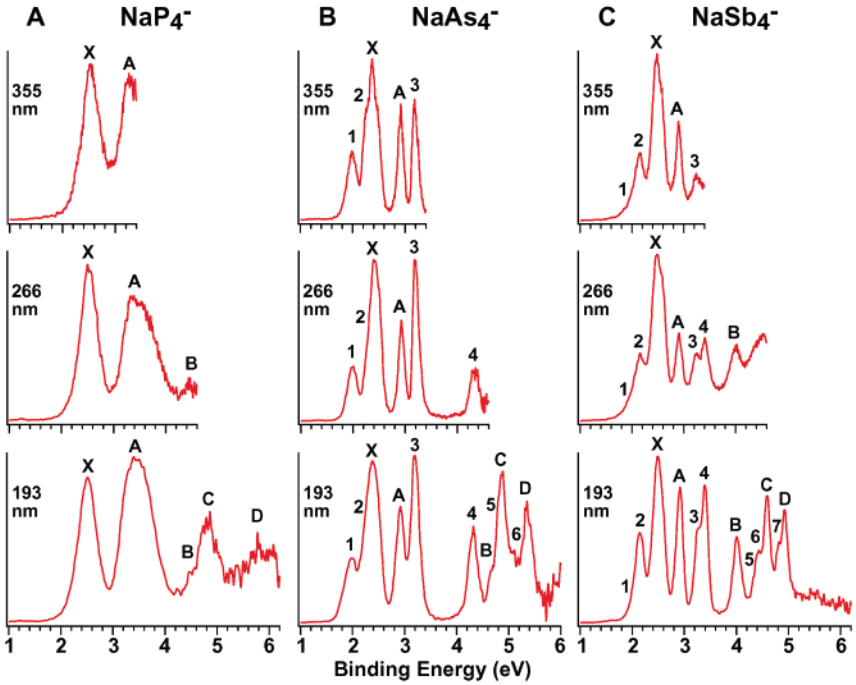

Figure 1. Photoelectron spectra of $NaPn_4^-$ (Pn = P, As, Sb) at 355 nm (3.496 eV), 266 nm (4.661 eV), and 193 nm (6.424 eV).

and a finite thermal effect. The ADE so estimated is 2.2 eV with a large uncertainty of ±0.1 eV. We should point out that all VDEs and ADEs were measured from the 355 nm spectra, which were better resolved. In general, several spectra were measured and calibrated to ensure consistency in the experimental data.

At 266 nm, the A band was shown to be very broad. As will be seen later (Table 1), the broad widths of the X and A bands are consistent with the fact they are due to detachment from degenerate MOs, resulting in Jahn−Teller distortions. A weak feature (B) was also discernible in the 266 nm spectrum at the high binding energy side. More features were revealed in the 193 nm spectrum. The high binding energy side of the 193 nm spectrum showed a poor signal-to-noise ratio due to the relatively weak NaP_4^- anion density and large background electron noise in this part of the spectrum. But the B feature could still be recognized, and two more features (C and D) were tentatively identified. The VDEs of all five features are listed in Table 1 and compared to values from theoretical calculations.

$NaAs_4^-$ and $NaSb_4^-$. The PES spectra of $NaAs_4^-$ and $NaSb_4^-$ were similar, but surprisingly, they appeared to be very different from that of NaP_4^-. Many more peaks were observed in the spectra of the two heavier $NaPn_4^-$ species, and the spectral features seemed to be much sharper compared to those of NaP_4^-. As will be shown later by comparing the experimental data and theoretical results, two isomers were in fact present for $NaAs_4^-$ and $NaSb_4^-$. The features labeled by the letters (X, A−D) were assigned to be from the main isomers, and they are similar to those of NaP_4^- in spectral patterns. The ADEs of the main isomers of $NaAs_4^-$ and $NaSb_4^-$ were estimated from the X features to be 2.3 eV for both species with a large uncertainty (±0.1 eV) due to the spectral congestions. The features labeled by the numbers (1−7) were assigned to be due to a low-lying isomer. The VDEs of the observed spectral features were determined from the peak maxima and are also given in Table 1.

The experimental data are combined and compared with the results of ab initio calculations, to elucidate the structure and bonding of the tetrapnictogen singly and doubly charged anions and assess their aromaticity and antiaromaticity.

Theoretical Results

Neutral Pn_4. We first calculated the known T_d structures of P_4, As_4, and Sb_4 using three different methods. The results of our calculations are compared with previous experimental data in Table 2. Our optimized geometries and calculated harmonic frequencies agree well with the available experimental data and with previously published ab initio results.[32,33] We expected that the accuracy of our calculations would be similar for other species considered here.

The neutral tetrapnictogens (Pn_4) are known to be tetrahedral molecules. However, in analogy with the corresponding prototypical antiaromatic C_4H_4 hydrocarbon molecule, we also evaluated the relative energies of the antiaromatic rectangular structures of Pn_4, which were known previously to be local minima.[33] We found that indeed the rectangular structures of P_4, As_4, and Sb_4 are local minima (see Figure 2 for As_4), although they are not perfectly planar (see Supporting Information, Figures 1S−3S and Tables S1 and S2). They have a small "butterfly"-type distortion (Figures

(28) Maxwell, L. R.; Hendricks, S. B.; Mosley, V. M. *J. Chem. Phys.* **1935**, *3*, 699.
(29) McDowell, R. S. *Spectrochim. Acta, Part A* **1971**, *27*, 773.
(30) Morino, J.; Ukaji, T.; Yto, T. *Bull. Chem. Soc. Jpn.* **1966**, *39*, 71.
(31) Brumbach, S. B.; Rosenblatt, G. M. *J. Chem. Phys.* **1972**, *56*, 3110.
(32) Zhang, H.; Balasubramanian, K. *J. Chem. Phys.* **1992**, *97*, 3437.
(33) Kobayashi, K.; Miura, H.; Nagase, S. *THEOCHEM* **1994**, *311*, 69.

Table 1. Experimental and Theoretical Vertical Electron Detachment Energies (VDE, eV) for $NaPn_4^-$ (Pn = P, As, Sb)

structure	obsd feature	VDE (expt)[a]	molecular orbital	VDE (theor)[b]
NaP_4^- (C_{4v})	X	2.52 (0.05)	3e	2.46 (0.88)
	A	3.3 (0.1)	2e	2.96 (0.88)
	B	4.6 (0.1)	$3a_1$	5.34 (0.80)
	C	4.9 (0.1)	$2a_1$	5.35 (0.77)
	D	5.9 (0.2)	$1b_1$	6.11 (0.87)
(C_{2v})			$3b_1$	1.93 (0.88)
			$5a_1$	2.09 (0.89)
			$2b_2$	3.03 (0.88)
			$1a_2$	4.65 (0.88)
			$4a_1$	5.03 (0.88)
			$2b_1$	5.19 (0.88)
$NaAs_4^-$ (C_{4v})	X	2.36 (0.03)	3e	2.43 (0.87)
	A	2.93 (0.03)	2e	3.02 (0.88)
	B	4.69 (0.06)	$3a_1$	4.73 (0.77)
	C	4.88 (0.05)	$2a_1$	4.98 (0.79)
	D	5.35 (0.05)	$1b_1$	5.51 (0.85)
(C_{2v})	1	1.99 (0.04)	$3b_1$	2.01 (0.87)
	2	2.24 (0.05)	$5a_1$	2.19 (0.87)
	3	3.18 (0.04)	$2b_2$	3.11 (0.88)
	4	4.33 (0.04)	$1a_2$	4.27 (0.88)
	5	4.66 (0.06)	$4a_1$	4.73 (0.87)
	6	5.08 (0.07)	$2b_1$	4.89 (0.87)
$NaSb_4^-$ (C_{4v})	X	2.48 (0.06)	3e	2.29 (0.87)
	A	2.90 (0.04)	2e	2.93 (0.88)
	B	4.01 (0.05)	$3a_1$	4.12 (0.76)
	C	4.59 (0.05)	$2a_1$	4.49 (0.78)
	D	4.93 (0.05)	$1b_1$	4.90 (0.85)
(C_{2v})	1	1.9 (0.1)	$3b_1$	1.97 (0.88)
	2	2.15 (0.05)	$5a_1$	2.17 (0.89)
	3	3.24 (0.05)	$2b_2$	2.99 (0.88)
	4	3.41 (0.05)	$1a_2$	3.87 (0.88)
	5	4.33 (0.05)	$4a_1$	4.27 (0.86)
	6	4.43 (0.05)	$2b_1$	4.42 (0.87)
	7	4.82 (0.05)	$3a_1$	4.79 (0.85)

[a] The numbers in the parentheses represent the experimental uncertainty. The adiabatic detachment energies for the C_{4v} isomers are 2.2 ± 0.1 eV for NaP_4^-, 2.3 ± 0.1 eV for $NaAs_4^-$, and 2.3 ± 0.1 eV for $NaSb_4^-$. [b] The VDEs were calculated at the OVGF/6-311+G(2df) (NaP_4^- and $NaAs_4^-$) and at the OVGF/CEP-121G+spd ($NaSb_4^-$) levels of theory. The first VDEs for the C_{4v} isomers at CCSD(T)/6-311+G(2df) are 2.40 eV for NaP_4^- and 2.42 eV for $NaAs_4^-$, and 2.32 eV for $NaSb_4^-$ (CCSD(T)/CEP-121G+spd). The numbers in the parentheses indicate the pole strength, which characterizes the validity of the 1-electron detachment picture. The calculated adiabatic detachment energies for the C_{4v} isomers are 2.20 eV for NaP_4^-, 2.26 eV for $NaAs_4^-$ (both at CCSD(T)/6-311+G(2df)), and 2.13 eV for $NaSb_4^-$ (CCSD(T)/CEP-121G+spd).

1S−3S). The relative energies of these isomers were found to be 59.0 kcal/mol (P_4), 50.2 kcal/mol (As_4), and 40.2 kcal/mol (Sb_4) higher than the corresponding tetrahedral structures (hereafter, we present all relative energies evaluated at our best level of theory). Moreover, P_4 and As_4 are not stable toward dissociation into two Pn_2 molecules, consistent with the destabilizing effects of antiaromaticity and the inability to observe these isomers experimentally. The similar isomer of Sb_4 was found to be slightly stable toward dissociation into two Sb_2 molecules (by 10.0 kcal/mol). While the distorted rectangular isomers of Pn_4 are certainly antiaromatic as it can be seen in Figure 3, they cannot be accessed experimentally.

Singly Charged Pn_4^-. Aromaticity and antiaromaticity were established for molecules with an even number of electrons. When a molecule has $4n + 2$ π-electrons it is aromatic, and when it has $4n$ electrons it is antiaromatic. Species with the odd number of π-electrons did not receive much attention so far. We believe that the molecules with odd numbers of electrons should be considered as antiaromatic because they have geometric distortions and reactivity similar to those of antiaromatic molecules. For example, the cyclic hydrocarbon $C_4H_4^-$ anion was calculated to be rectangular.[34] The singly charged tetrapnictogen anions (Pn_4^-) could also potentially exhibit antiaromaticity. However, as shown in Figure 2 for As_4^-, we found all three Pn_4^- species to be more stable at the "roof" (C_{2v}, $^2B_1$) structures at all three levels of theory (Tables S3−S5 and Figures 1S−3S). The roof structure is related to the tetrahedral structure: upon electron attachment, one edge of the tetrahedron is elongated by about 0.6 Å yielding the roof structure. We also found that a rectangular (D_{2h}, $^2B_{1g}$) structure is a local minimum for all three tetrapnictogen anions at all three levels of theory. The D_{2h} ($^2B_{1g}$) structure is similar to the antiaromatic D_{2h} ($^2B_{1g}$) structure of $C_4H_4^-$. The difference calculated for the Pn_4^- rectangular edges is 0.12 Å, same as in $C_4H_4^-$.[34] The antiaromatic rectangular isomer was found to be very close in energy to the ground state "roof" structure. The relative energies were found to be 5.0 kcal/mol (P_4^-), 5.9 kcal/mol (As_4^-), and 5.6 kcal/mol (Sb_4^-). Therefore, the antiaromatic rectangular structure should be a viable isomer.

To our surprise, we found another local minimum [only at the MP2 and CCSD(T) levels of theory]: a quasiplanar rhombus (butterfly) Pn_4^- (C_{2v}, $^2B_1$) structure (Figure 2). The deviation from the planar rhombus structure is very small (about 0.1 Å), and after the ZPE averaging, the effective structure is actually planar. The quasiplanar rhombus structure can also be considered to be antiaromatic even though it has no analogy in hydrocarbons. Calculated molecular parameters for all three Pn_4^- structures are summarized in the Supporting Information (Figures 1S−3S and Tables S4−S6). The calculated energies of the rhombus structure relative to the roof structure were found to be 5.6 kcal/mol for P_4^-, 6.9 kcal/mol for As_4^-, and 6.3 kcal/mol for Sb_4^-. Therefore, under normal experimental conditions, the antiaromatic rectangular and rhombus structures of Pn_4^- are not accessible, and only the global minimum roof structures can be made, as shown in previous PES studies on several Pn_4^- species.[35−38]

Doubly Charged Pn_4^{2-}. Upon further electron attachment to the "roof" structure and to the rhombus or rectangular isomers of Pn_4^-, the resulting doubly charged Pn_4^{2-} species were found again to have a roof isomer (Figure 2 and Table 3) and a perfect square-planar isomer (Figure 2 and Table 4). The square-planar structures of P_4^{2-}, As_4^{2-}, and Sb_4^{2-} were found to be the global minima and possess the same set of π-MOs as the reference $C_4H_4^{2-}$ molecule, as shown in Figure 3 for As_4^{2-}. Thus, they are unquestionably aromatic

(34) Piocos, E. A.; Werst, D. W.; Trifunac, A. D.; Eriksson, L. A. *J. Phys. Chem.* **1996**, *100*, 8408.
(35) Jones, R. O.; Gantefor, G.; Hunsiker, S.; Pieperhoff, P. *J. Chem. Phys.* **1995**, *103*, 9549.
(36) Lippa, T. P.; Xu, S.-J.; Lyapustina, S. A.; Nilles, J. M.; Bowen, K. H. *J. Chem. Phys.* **1998**, *109*, 10727.
(37) Polak, M. L.; Gerber, G.; Ho, J.; Lineberger, W. C. *J. Chem. Phys.* **1992**, *97*, 8990.
(38) Gausa, M.; Kaschner, R.; Seifert, S.; Faehrmann, J. H.; Lutz, H. O.; Meiwess-Broer, K.-H. *J. Chem. Phys.* **1996**, *104*, 9719.

Table 2. Calculated Molecular Properties of the T_d Structure of P_4, As_4, and Sb_4

P_4, $^1A_1$	B3LYP/6-311+G*	MP2(full)/6-311+G*	CCSD(T)/6-311+G*	expt
E_{tot}, au	−1365.53549	−1363.92797	−1363.48506	
R(P−P), Å	2.220	2.207	2.219	2.21 ± 0.02[a]
$\omega_1(a_1)$, cm^{-1}	597	606	598	604.4[b]
$\omega_2(e)$, cm^{-1}	399	350	352	361[b]
$\omega_3(t_2)$, cm^{-1}	452	451	448	461.5[b]

As_4, $^1A_1$	B3LYP/6-311+G*	MP2/6-311+G*	CCSD(T)/6-311+G*	expt
E_{tot}, au	−8943.62331	−8936.70826	−8937.20573	
R(As−As), Å	2.463	2.474	2.482	2.435 ± 0.004[d]
$\omega_1(a_1)$, cm^{-1}	348	347	c	344 ± 1.5[e]
$\omega_2(e)$, cm^{-1}	202	196	c	210 ± 2.5[e]
$\omega_3(t_2)$, cm^{-1}	258	254	c	235 ± 3.5[e]

Sb_4, $^1A_1$	B3LYP/CEP-121G+spd	MP2/CEP-121G+spd	CCSD(T)/CEP-121G+spd
E_{tot}, au	−21.92479	−21.65223	−21.69162
R(Sb−Sb), Å	2.848	2.858	2.873
$\omega_1(a_1)$, cm^{-1}	238	236	231
$\omega_2(e)$, cm^{-1}	134	131	131
$\omega_3(t_2)$, cm^{-1}	175	172	170

[a] Reference 26. [b] Reference 27. [c] Frequencies have not been calculated at this level of theory. [d] Reference 28. [e] Reference 29.

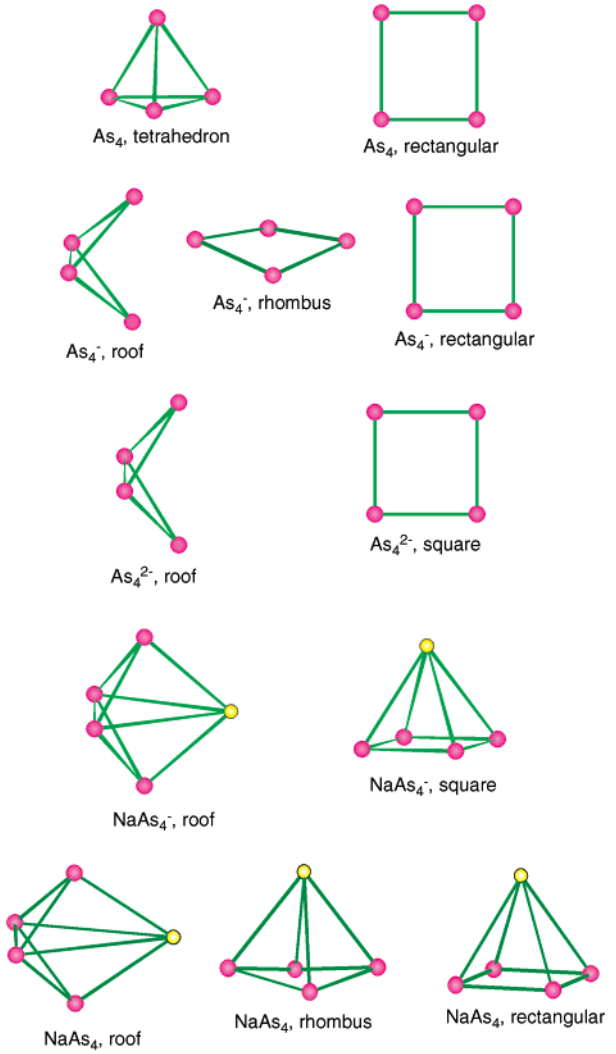

Figure 2. Optimized structures of As_4, As_4^-, As_4^{2-}, $NaAs_4^-$, and $NaAs_4$ at the MP2/6-311+G* level of theory. See Supporting Information for structural details as well as data on the corresponding P- and Sb-containing species.

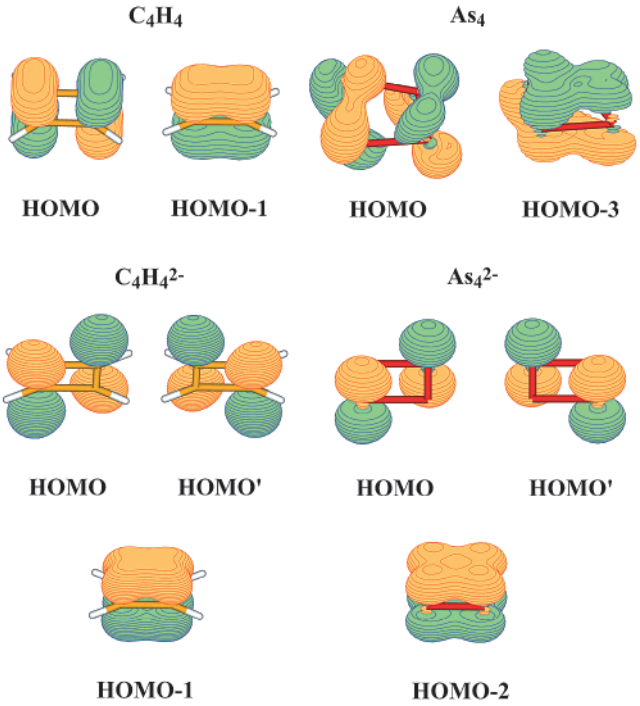

Figure 3. Molecular structure and molecular orbital pictures of C_4H_4, As_4, $C_4H_4^{2-}$, and As_4^{2-}.

inorganic molecules. The roof isomer of the tetrapnictogen dianions was found to be 18.1 kcal/mol (P_4^{2-}), 14.2 kcal/mol (As_4^{2-}), and 10.7 kcal/mol (Sb_4^{2-}) higher in energy than the corresponding aromatic square-planar structure. Square-planar Sb_4^{2-} and Bi_4^{2-} dianions are well-known building blocks of solid materials.[39,40] Our calculated Sb−Sb bond length (2.82−2.84 Å) for the isolated Sb_4^{2-} dianion (Table 4) and in the $NaSb_4^-$ (C_{4v}, $^1A_1$) anion (Table 5) are in reasonable agreement with the experimental data, 2.75 Å in the (2,2,2-crypt-K^+)$_2Sb_4$ crystal.[39]

The "roof" P_4^{2-} structure was also found as a building block in the [{Cp‴(OC)$_2$Fe}$_2$(η-μ^1:μ^1-P_4)] (Cp‴ = C_5H_2-Bu^t_3-1,2,4) crystal.[41] Our calculated parameters for the P_4^{2-}

(39) Critchlow, S. C.; Corbett, J. D. *Inorg. Chem.* **1984**, *23*, 770.
(40) Cisar, A.; Corbett, J. D. *Inorg. Chem.* **1977**, *16*, 2482.
(41) Scherer, O. J.; Hilt, T.; Wolmershauser, G. *Organometallics* **1998**, *17*, 4110.

Table 3. Calculated Molecular Properties of the Roof Structure of P_4^{2-}, As_4^{2-}, and Sb_4^{2-}

P_4^{2-}, C_{2v}, $^1A_1$	B3LYP/6-311+G*	MP2(full)/6-311+G*	CCSD(T)/6-311+G*
E_{tot}, au	−1365.43970	−1363.79636	−1363.35813
$R(P_1-P_2)$, Å	2.158	2.143	2.159
$R(P_1-P_3)$, Å	2.280	2.243	2.266
$R(P_3-P_4)$, Å	3.321	3.246	3.260
$\omega_1(a_1)$, cm^{-1}	542	565	548
$\omega_2(a_1)$, cm^{-1}	386	397	386
$\omega_3(a_1)$, cm^{-1}	206	206	199
$\omega_4(a_2)$, cm^{-1}	235	254	240
$\omega_5(b_1)$, cm^{-1}	388	414	399
$\omega_6(b_2)$, cm^{-1}	297	315	304

As_4^{2-}, C_{2v}, $^1A_1$	B3LYP/6-311+G*	MP2/6-311+G*	CCSD(T)/6-311+G*
E_{tot}, au	−8943.54371	−8937.05943	−8937.10748
$R(As_1-As_2)$, Å	2.403	2.410	2.422
$R(As_1-As_3)$, Å	2.516	2.502	2.525
$R(As_3-As_4)$, Å	3.603	3.535	3.568
$\omega_1(a_1)$, cm^{-1}	314	323	*a*
$\omega_2(a_1)$, cm^{-1}	218	224	*a*
$\omega_3(a_1)$, cm^{-1}	102	97	*a*
$\omega_4(a_2)$, cm^{-1}	134	(1395)[b]	*a*
$\omega_5(b1)$, cm^{-1}	226	237	*a*
$\omega_6(b2)$, cm^{-1}	176	(694)[b]	*a*

Sb_4^{2-}, C_{2v}, $^1A_1$	B3LYP/ CEP-121G+spd	MP2/ CEP-121G+spd	CCSD(T)/ CEP-121G+spd
E_{tot}, au	−21.87183	−21.57282	−21.61712
$R(Sb_1-Sb_2)$, Å	2.789	2.798	2.815
$R(Sb_1-Sb_3)$, Å	2.903	2.891	2.919
$R(Sb_3-Sb_4)$, Å	4.177	4.103	4.129
$\omega_1(a_1)$, cm^{-1}	212	217	209
$\omega_2(a_1)$, cm^{-1}	146	149	144
$\omega_3(a_1)$, cm^{-1}	65	62	59
$\omega_4(a_2)$, cm^{-1}	99	108	99
$\omega_5(b_1)$, cm^{-1}	122	129	123
$\omega_6(b_2)$, cm^{-1}	158	164	156

[a] Frequencies have not been calculated at this level of theory. [b] Symmetry broken problem.

Table 4. Calculated Molecular Properties of the Square-Planar Aromatic Structure of P_4^{2-}, As_4^{2-}, and Sb_4^{2-}

P_4^{2-}, D_{4h}, $^1A_{1g}$	B3LYP/6-311+G*	MP2(full)/6-311+G*	CCSD(T)/6-311+G*
E_{tot}, au	−1365.47546	−1363.83297	−1363.38952
R(P−P), Å	2.189	2.168	2.177
$\omega_1(a_{1g})$, cm^{-1}	466	475	474
$\omega_2(b_{1g})$, cm^{-1}	306	290	301
$\omega_3(b_{2g})$, cm^{-1}	483	498	494
$\omega_4(b_{2u})$, cm^{-1}	201	159	162
$\omega_5(e_u)$, cm^{-1}	404	448	417

As_4^{2-}, D_{4h}, $^1A_{1g}$	B3LYP/6-311+G*	MP2/6-311+G*	CCSD(T)/6-311+G*
E_{tot}, au	−8943.56945	−8937.08856	−8937.13007
R(As−As), Å	2.419	2.425	2.430
$\omega_1(a_{1g})$, cm^{-1}	269	265	*a*
$\omega_2(b_{1g})$, cm^{-1}	162	148	*a*
$\omega_3(b_{2g})$, cm^{-1}	275	277	*a*
$\omega_4(b_{2u})$, cm^{-1}	100	85	*a*
$\omega_5(e_u)$, cm^{-1}	233	265	*a*

Sb_4^{2-}, D_{4h}, $^1A_{1g}$	B3LYP/ CEP-121G+spd	MP2/ CEP-121G+spd	CCSD(T)/ CEP-121G+spd
E_{tot}, au	−21.89260	−21.59589	−21.63418
R(Sb−Sb), Å	2.801	2.810	2.822
$\omega_1(a1_g)$, cm^{-1}	182	178	177
$\omega_2(b_{1g})$, cm^{-1}	96	88	92
$\omega_3(b_{2g})$, cm^{-1}	187	186	184
$\omega_4(b_{2u})$, cm^{-1}	60	52	51
$\omega_5(e_u)$, cm^{-1}	163	183	161

[a] Frequencies have not been calculated at this level of theory.

isolated dianion [$R(P_1-P_4) = 3.260$ Å, $R(P_1-P_{2,3}) = 2.266$ Å, $R(P_2-P_3) = 2.159$ Å, and $R(P_4-P_{2,3}) = 2.266$ Å] were found to be in reasonable agreement with the experimental data [$R(P_1-P_4) = 2.96$ Å, $R(P_1-P_{2,3}) = 2.217(3)$ Å, $R(P_2-P_3) = 2.151(2)$ Å, and $R(P_4-P_{2,3}) = 2.203(3)$ Å on average]. We also found that the extra charges in the roof structure are primarily located on the P atoms of the long P···P edge, which fits perfectly into the [{Cp‴(OC)$_2$Fe}(η-μ^1:μ^1-P_4)] crystal structure.

Alkali-Stabilized Pn_4^{2-}: $Na^+Pn_4^{2-}$. One strategy to access the antiaromatic rectangular and rhombus structures of Pn_4^- is to detach an electron from the aromatic square Pn_4^{2-}. Because of the large geometry changes and different electronic configurations between the square-planar structure of Pn_4^{2-} and the "roof" structure of Pn_4^-, electron detachment from a square Pn_4^{2-} can only reach the potential energy surfaces of the rectangular and rhombus Pn_4^-, thus finessing thermodynamics in the process.

However, the Pn_4^{2-} doubly charged anions are not electronically stable species and cannot be produced in the gas phase for an experimental PES investigation. Our strategy to reach the antiaromatic structures of Pn_4^- was then to use Na^+ to stabilize the Pn_4^{2-} dianions, as we had done previously to stabilize the Al_4^{2-} aromatic cluster in $NaAl_4^-$ ($Na^+Al_4^{2-}$)[5] or the common inorganic dianion SO_4^{2-} in $NaSO_4^-$ ($Na^+SO_4^{2-}$).[42] The alkali cation will primarily stabilize Pn_4^{2-} electrostatically as a spectator without altering substantially their electronic and geometrical structures.

The global minimum structure of $NaPn_4^-$ was found to be square-pyramidal, consisting of an Na^+ ion coordinated to a Pn_4^{2-} square (Figure 2 and Table 5). The "roof"-like structure was found to be local minima for Pn_4^{2-} and $NaPn_4^-$ (its molecular parameters are summarized in Figures 1S−3S and Table S6 in the Supporting Information). We found that the "roof" isomer was higher than the pyramidal one by 9.8 kcal/mol for NaP_4^-, 6.5 kcal/mol for $NaAs_4^-$, and 2.4 kcal/mol for $NaSb_4^-$. It is interesting to note that the roof isomer becomes energetically more competitive with the pyramidal structure for the heavier $NaPn_4^-$ species. However, for the neutral $NaPn_4$ ($Na^+Pn_4^-$) species, we found the "roof"-like structure to be the global minimum, though it possesses low-lying isomers that are derivatives of the rectangular and rhombus structures of Pn_4^- (Figure 2). The results for $NaPn_4$ ($Na^+Pn_4^-$) are consistent with those of bare Pn_4^-, again indicating that the cation is only a spectator that does not affect the electronic structure of the anions. The optimized geometries, vibrational frequencies, and relative energies agreed well at the three levels of theory used in this work for all species. Detailed theoretical data on $NaPn_4$ are summarized in the Supporting Information (Figures 1S−3S and Tables S7−S9).

Interpretation of the PES Spectra and Comparison with Theoretical Calculations. As we showed previously,[4,5,43−45] combining ab initio calculations and PES experi-

(42) Wang, X. B.; Ding, C. F.; Nicholas, J. B.; Dixon, D. A.; Wang, L. S. *J. Phys. Chem. A* **1999**, *103*, 3423.
(43) Li, X.; Wang, L. S.; Boldyrev A. I.; Simons, J. *J. Am. Chem. Soc.* **1999**, *121*, 6033.
(44) Li, X.; Zhang, H. F.; Wang, L. S.; Kuznetsov, A. E.; Cannon, N. A.; Boldyrev, A. I. *Angew. Chem., Int. Ed.* **2001**, *40*, 1867.
(45) Boldyrev, A. I.; Wang, L. S. *J. Phys. Chem. A* **2001**, *105*, 10759.

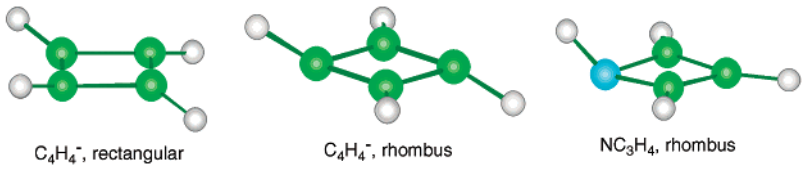

Figure 4. Optimized structures of $C_4H_4^-$ and NC_3H_4 at the MP2/6-311+G* level of theory. See Supporting Information for structural data.

ments provides a valuable means to understand the structures and chemical bonding of small clusters. This is particularly true for clusters containing less than six atoms of the main group elements because their possible structures and spin states can be searched reasonably accurately and timely with the available computational facilities. Our prior works on a number of small Al-containing clusters have shown that calculated VDEs from the lowest energy isomer usually give good agreement with experimental PES data, allowing several clusters with novel structures and chemical bonding to be characterized. For the $NaPn_4^-$ species, our theoretical results showed that the ground state is the pyramidal structure (C_{4v}) with a low-lowing "roof"-like isomer (C_{2v}) (Figures 2 and 1S−3S). Theoretical VDEs were calculated for both isomers (Table 1) and are used to interpret the experimental observations. Because both isomers of $NaPn_4^-$ are closed shell species, each occupied MO is expected to yield one PES feature, whose theoretical VDE is listed in Table 1. We found that the VDEs of the C_{2v} low-lying isomer are lower than those of the C_{4v} ground state for all three $NaPn_4^-$ anions.

NaP_4^-. The calculated VDEs of the C_{4v} isomer of NaP_4^- are in reasonable agreement with the PES data. In particular, the VDE of the ground state transition is in very good agreement with the experimental result for the X band. The HOMO and HOMO − 1 of the C_{4v} NaP_4^- are both doubly degenerate, which would result in Jahn−Teller distortions in the final neutral states, consistent with the broad spectra observed for the X and A bands in the PES spectra of NaP_4^- and the optimized structures of the neutral NaP_4 (Figure 1S). The VDE for the ground state transition of the C_{2v} isomer of NaP_4^- was calculated to be 1.93 eV (Table 1). No spectral feature was observed in this energy range in the PES spectra, suggesting that the C_{2v} isomer was negligible in the experiment. This is consistent with the energetics of the two isomers. Our calculation showed that the C_{2v} isomer is 9.8 kcal/mol higher in energy than the ground state C_{4v} structure.

$NaAs_4^-$ and $NaSb_4^-$. The PES spectra of the two heavier $NaPn_4^-$ anions appeared to be much more complicated with many more resolved features. Our calculations indicate that the C_{2v} isomer becomes energetically competitive with the C_{4v} ground states for these two species, suggesting the possibility that the C_{2v} isomer might be significantly populated in the cluster beams. Indeed, a relatively weak peak was observed in the low binding energy side in the spectra of both $NaAs_4^-$ and $NaSb_4^-$. We assigned these weak features to be due to the C_{2v} isomer. Our calculated VDE for the ground state of both isomers is in good agreement with the experimental data. The calculated VDE for the HOMO − 1 of the C_{4v} ground state of both $NaAs_4^-$ and $NaSb_4^-$ is well separated from the ground state transition and could be assigned to the A band in each case. However, the calculated VDEs for the deeper MOs of the C_{4v} ground states and those of the C_{2v} isomers are rather close, making the spectral identification rather challenging. Thus, the spectral assignments given in Table 1 should be viewed as tentative. However, the reasonable overall agreement between the experimental data and the calculated VDEs lends some credence to the assignments.

Making Antiaromatic Inorganic Molecules: Photodetachment of $NaPn_4^-$. We found that the MOs of $NaPn_4^-$ and Pn_4^{2-} are almost identical, as was the case for $NaAl_4^-$ and Al_4^{2-}.[5] More importantly, the global minimum structures of all the $NaPn_4^-$ species contain the aromatic square Pn_4^{2-} dianion. Hence, the lowest detachment energy channel of the C_{4v} $NaPn_4^-$, because of the removal of one π-electron (3e HOMO), should lead to the first antiaromatic inorganic species. More importantly, the experimental ADEs of the square-pyramidal $NaPn_4^-$ and the calculated ADEs between the square-pyramidal $NaPn_4^-$ and the rectangular $NaPn_4$ are in excellent agreement (see the footnotes of Table 1). This confirmed that indeed the antiaromatic forms of Pn_4^- have been produced by detaching an electron from the HOMO of $NaPn_4^-$ (Pn = P, As, Sb). The resulting neutral $NaPn_4$ species have two pyramidal structures with a rectangular and a rhombus base, which are very close in energy, and both may be reached in the photodetachment.

Antiaromatic Structures for $C_4H_4^-$ and NC_3H_4. In our search for the Pn_4^- global minimum, we found two antiaromatic structures: rectangular and rhombus. While the rectangular structure for $C_4H_4^-$ was predicted in the previous work,[34] the rhombus structure was not considered. Because we use the $C_4H_4^-$ hydrocarbon molecule as our reference of antiaromaticity, we decided to further investigate its geometries including both the rectangular and the rhombus structures. We optimized geometries for both structures using the B3LYP/6-311++G**, MP2/6-311++G**, and CCSD(T)/6-311++G** levels of theory. At all three levels of theory, the optimized geometric parameters were found to be in good agreement with each other. The optimized structures of $C_4H_4^-$ are shown in Figure 4, and geometric parameters and harmonic frequencies are presented in the Supporting Information (Figure 4S and Table S10). While the cyclic carbon framework is perfectly planar in both structures, the hydrogen atoms were found to be slightly out of plane (Figure 4). At the B3LYP/6-311++G** level of theory, we found that the rectangular structure is a true minimum, but the rhombus structure was found to be a first-order saddle point with the imaginary mode leading toward the rectangular structure, similar to our findings for P_4^- and As_4^-. However, at the other two levels of theory, we found that both the rectangular and the rhombus structures are minima with the former one being slightly more stable. The

Hartree−Fock wave functions were found to be dominant in both cases: C_{HF}(rectangular) = 0.97 and C_{HF}(rhombus) = 0.96 in the CASSCF(9,8)/6-311++G** expansion. To test further the existence of the rhombus structure in organic molecules, we tested a neutral heterocyclic NC_3H_4 radical (Figures 4 and 4S). Surprisingly, we only found the rhombus minimum structure for NC_3H_4 (Table S11). On the basis of our calculations, we confirmed that hydrocarbons can also possess the rhombus antiaromatic structures.

Discussion

From Antiaromatic Pn_4 to Aromatic Pn_4^{2-}. From our calculations, we observed that there is a competition between two types of structures for the $Pn_4^{2-/1-/0}$ species: the first one is related to the tetrahedral structure of Pn_4, and the second one is the quasiplanar antiaromatic rectangular structure of Pn_4. When the charge on Pn_4 is zero, the tetrahedral structure is substantially more stable (59.0 kcal/mol for P_4, 50.2 kcal/mol for As_4, and 40.2 kcal/mol for Sb_4) than the rectangular one, which is in agreement with the antiaromatic nature of the latter. Very high calculated relative energies of the antiaromatic structure make their experimental observation impossible.

When two electrons are added to the Pn_4 species, the resulting Pn_4^{2-} doubly charged anion was found to have two low-lying isomers. The lowest structure was found to be the aromatic square-planar structure with the "roof" structure being higher in energy: 18.1 kcal/mol for P_4^{2-}, 14.2 kcal/mol for As_4^{2-}, and 10.7 kcal/mol for Sb_4^{2-}. These results clearly demonstrated the influence of the aromaticity and antiaromaticity on the relative stability of the $Pn_4^{2-/-/0}$ isomers. Upon addition of electrons to the third π-MO, the relative stability of the planar (or quasiplanar) structures is increasing very fast, changing the global minimum structure from the 3D tetrahedron in Pn_4 to the square-planar structure in Pn_4^{2-}. We also would like to point out that the relative stability of the aromatic structure relative to the T_d structure is decreasing along the $P_4^{2-} \rightarrow As_4^{2-} \rightarrow Sb_4^{2-}$ series because of the decreasing strength of the π-bond along the same series.

Gascoin and Sevov[46] recently published a synthesis and characterization of A_4Pn_4-type salts (A = K, Rb, Cs and Pn = As, Sb, Bi), which contain isolated Pn_4^{4-} species with zigzag structures. We believe that, upon further electron attachments to the planar square Pn_4^{2-} structure, the additional pair of electrons filled up the antibonding σ-MOs, resulting in the rupture of the cyclic structure and the formation of the zigzag structure.

5 π-Electron Pn_4^- Systems: Aromatic or Antiaromatic? Upon attachment of one electron to Pn_4, the roof (C_{2v}, $^2B_1$) structure originated from the tetrahedron was found still to be the most stable. This result agrees with previous theoretical and experimental data.[35−38] The major geometric change from the T_d to the C_{2v} structure occurs in the elongation of one Pn−Pn edge by about 0.6 Å. Additionally, we found two new isomers: a rectangular structure and a quasiplanar rhombus structure (Figures 2 and 1S−3S). The planar Pn_4^- species now only have 5 π-electrons and fall between the $(4n + 2)$ and $4n$ Hückel electron rules for aromaticity and antiaromaticity. However, on the basis of the structural characteristics of typical antiaromatic molecules, we propose that the rectangular 5 π-electron Pn_4^- species should be considered antiaromatic, just as in the case of the typical organic molecule, $C_4H_4^-$. We computationally predicted that $C_4H_4^-$ possesses two antiaromatic isomers: rectangular and rhombus (Figure 4). Thus, both antiaromatic isomers are viable for $C_4H_4^-$. The rhombus antiaromatic structure may be rationalized by examining the nature of the HOMO of Pn_4^{2-}. It consists of a degenerate pair of π-orbitals composed of p_π-atomic orbitals from atoms at opposite corners of the square (Figure 3). Removal of 1 electron from the HOMO breaks the symmetry, and geometry relaxation can lead either to a rhombus or a rectangular structure in Pn_4^-. Occupation of the third π-MO in both antiaromatic structures by 1 electron leads to further stabilization relative to the roof structure. The antiaromatic Pn_4^- structures were found to be less stable by 6 kcal/mol relative to the ground state "roof" structure.

The characterization of the rectangular antiaromatic inorganic $NaPn_4$ ($Na^+Pn_4^-$) species helps firmly establish the aromaticity concept in inorganic chemistry. Furthermore, many rectangular and rhombus structural units exist in inorganic materials, and their structure and bonding may be understood on the basis of aromaticity and antiaromaticity. Finally, the finding of the antiaromatic rhombus structure in the $C_4H_4^-$ and NC_3H_4 species extended this new peculiar antiaromatic structure from inorganic into organic chemistry.

Conclusions

In summary, we obtained the photoelectron spectra of a series of tetrapnictogen species, $Na^+Pn_4^{2-}$ (Pn = P, As, Sb), at various photon energies and investigated their chemical structure and bonding using several levels of theory. Good agreement was achieved between the experimental PES data and the theoretical calculations, allowing us to characterize the structures and bonding of these new molecular species. We presented theoretical and experimental evidence that the $Na^+Pn_4^{2-}$ tetrapnictogen anions contain an aromatic Pn_4^{2-} dianion and the $Na^+Pn_4^-$ neutral species contain an antiaromatic Pn_4^- anion. Our conclusions on aromaticity and antiaromaticity were derived on the basis of molecular orbital analyses and verified by the experimental photodetachment spectra of $Na^+Pn_4^{2-}$. Interestingly, we found two types of antiaromatic structures, the conventional rectangular one and a new peculiar rhombus one. The existence of the antiaromatic rhombus structure in the $C_4H_4^-$ and NC_3H_4 species extended this new antiaromatic structure from the domain of inorganic clusters into organic chemistry.

Acknowledgment. The theoretical work was done at Utah State University and was supported by the donors of the Petroleum Research Fund, administered by the American Chemical Society (Grant ACS-PRF# 38242-AC6). The experimental work done at Washington was supported by

(46) Gascoin, F.; Sevov, S. C. *Inorg. Chem.* **2001**, *40*, 5177.

the National Science Foundation (Grant CHE-9817811) and performed at the W. R. Wiley Environmental Molecular Sciences Laboratory, a national scientific user facility sponsored by DOE's Office of Biological and Environmental Research and located at Pacific Northwest National Laboratory, which is operated for DOE by Battelle.

Supporting Information Available: Ab initio calculated geometric parameters and harmonic frequencies of all considered species (at B3LYP/6-311+G*, MP2/6-311+G* and CCSD(T)/6-311+G*) (Figures 1S−4S and Tables S1−S11). This material is available free of charge via the Internet at http://pubs.acs.org.

IC020426+